Caspian Journal of Environmental Sciences
Online ISSN: 1735-3866
Print ISSN: 1735-3033

Preparation and characterization of cadmium (ll), zinc (ll) and copper (ll) ion complexes using new triazene ligands and study of their biological activity

Haneen Sadi Hussein*, Mohammad Hamid Said, Ahmed Hassan Shantaf

University of Babylon, Chemistry Department, College of Science for Women, Iraq

** Corresponding author's Email: haneenbeati33@gmail.com*

ABSTRACT

The synthesis of novel ligand was disclosed in this study. This ligand was synthesized from reaction between 4-amino anti pyrene and 6-amino penicillanic acid by triazene reaction. The ligand was identified by FT-IR, UV-Visible, HNMR, Mass spectroscopy reacting the ligand with salts of transition metals Cu, Zn, Cd (II) complexes and gave octahedral, hybridization sp3d2 complexes with a molar ratio (1:2) M:L Magnetic Para-Di complexes were produced using amoral ratio of metal chloride to ligand spectroscopic data used to establish the identity of ligand of their corresponding complexes by FT-IR, UV-VIS, atomic absorption, magnetic susceptibility and conductivity. The ligand and its complex exhibited biological activity. It gave good results in inhibiting gram positive *Streptococcus* bacteria.

Keyword: Triazene, 6-amino penicillanic acid, 4-amino anti pyrene, Biological activity.
Article type: Research Article.

INTRODUCTION

Aromatic triazene compounds (N3RR′) have a significant impact on man-made and pharmaceutical chemistry (Ayakar & Yadav 2019). Until recently, the chemistry of phenyl alkenyl triazene remained mostly unknown. After the past five years have passed, it has become clear that phenyl and alkenyl triazene are very remarkable molecules with a distinct element, the active component of these substances is represented by the triazene group (Suleymanov & Kay 2021), triazene group, and are used in the treatment of cancer due to their low toxicity and kinetic properties powerful pharmacological (Francisco *et al.* 2019). It consists of three adjacent nitrogen atoms and is responsible for the chemical, physical and antitumor properties of the molecule (Marchesi *et al.* 2007). Penicillin, including 6-aminopenicillin is a chemical molecule used as a precursor in the manufacture of lactam antibiotics. Natural penicillin G remains the most common commercial source of 6-APA penicillin scheme (Fig. 1) and it is also a semi-synthetic penicillin produced from 6-APA; It is a member of the penicillin family of antibiotics (Patrick 2017) and one of the most important and widely used one. Beecham scientists at Brock ham Park, Surrey, discovered a mechanism for obtaining 6-APA from the form of penicillin (Fig. 1) in 1958 (Batchelor *et al.* 1959). It has a beta-lactam in its structure (Hui-nan *et al.* 2011; Zana Ibraimi *et al.* 2013). In addition, it is used to treat and prevent bacterial infections caused by microorganisms. It has bactericidal activity and is commonly used against both Gram-positive and Gram-negative bacteria. These kinds of antibiotics inhibit the bacterial cell wall (Naz & Iqbal 2011; Imam Pasha *et al.* 2012).

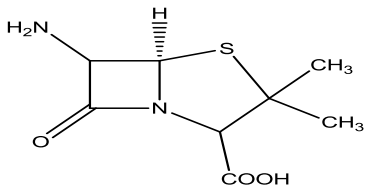

(5*R*)-6-amino-3,3-dimethyl-7-oxo-4-thia-1-azabicyclo[3.2.0]heptane-2-carboxylic acid

Fig. 1. The 6-amino penicillanic acid.

Caspian Journal of Environmental Sciences, Vol. 22 No. 3 pp. 663-672 Received: Feb. 08, 2024 Revised: May 17, 2024 Accepted: June 23, 2024
DOI: 10.22124/CJES.2023.6764

Publisher: University of Guilan

MATERIALS AND METHODS

Experimental part

chemicals

All chemicals were analytical used as received, metal salt, $CuCl_2.2H_2O$, $CdCl_2,2.2H_2O$, $ZnCl_2$, 6-amino penicillanic acid (98%), 4-aminoanti pyrene, Ethanol Absolut (99%).

Synthesis of ligand

2.6 g of 1 mole of 4-amioanti pyrene was dissolved in 4 mL of HCl and 8 mL of distal water. The mixtures cooled to 0 °C, and 0.6 g DW of sodium nitrite was added dropwise while stirring continuously. After leaving the solution for 30 min to stabilize, 2g of 6-APA (Na_2CO_3, 3 g dissolved in 6 mL DW) was added. A yellow precipitate was produced, filtered and recrystallized using 1:1 ethanol: water compound (Fig. 2).

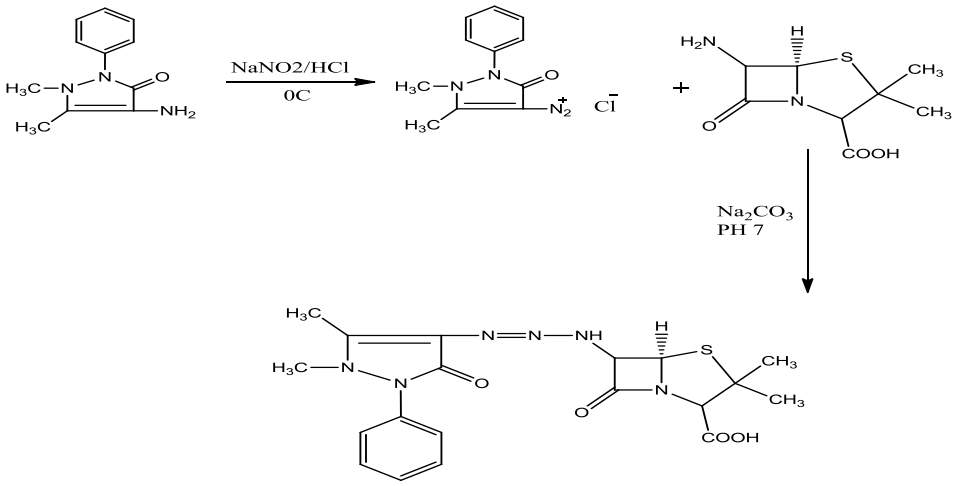

Fig. 2. Synthesis of ligand.

Synthesis of complexes

A round flask of 15 mL was taken and the prepared ligand was placed and dissolved in ethanol 15 mL and metal salts were added to it including $CdCl_2.2H_2O$, $CuCl_2.2H_2O$ and $ZnCl_2$ (1 mol including 0.1 g, 0.16 g, 0.2 g respectively; Fig. 3). After 3 hours of refluxing, the colourful complexes slowly formed and recrystallized from 99% ethanol.

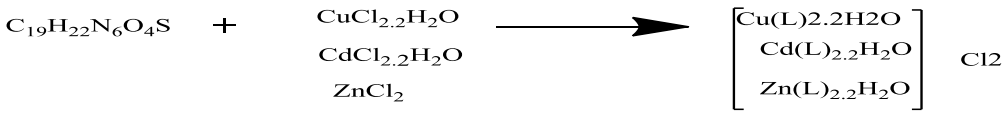

Fig. 3. Synthesis of complexes.

The physical properties are explained in the Table 1.

Table 1. The Physical properties of complex.

Compound	Color	Yield (%)	M.P	M. Wt
			C	
L	Brown	70	101	430
$[Zn(L)_2(H_2O)_2]Cl_2$	Brown	60	124	959
$[Cd\ (L)_2(H_2O)_2]Cl_2$	yellow	78	130	1008
$[Cu\ (L)_2(H_2O)_2]Cl_2$	green	70	110	961

RESULTS AND DISCUSSION

Mass spectroscopy

It was observed in the mass spectrum that a peak appears when this peak is attributed to the parent molecular ion (431) in Fig. 4 which corresponds to the proposed molecular formula of the bond. The spectrum recorded other peaks that correspond to the graph. The mass spectrum of the bonds is shown in Table 2. The fissions that occurred are shown.

Table 2. Fragmentation of ligand.

M/z	Abundance
97	64
102	48
28	155
15	158
48	252
38	260
15	431.06

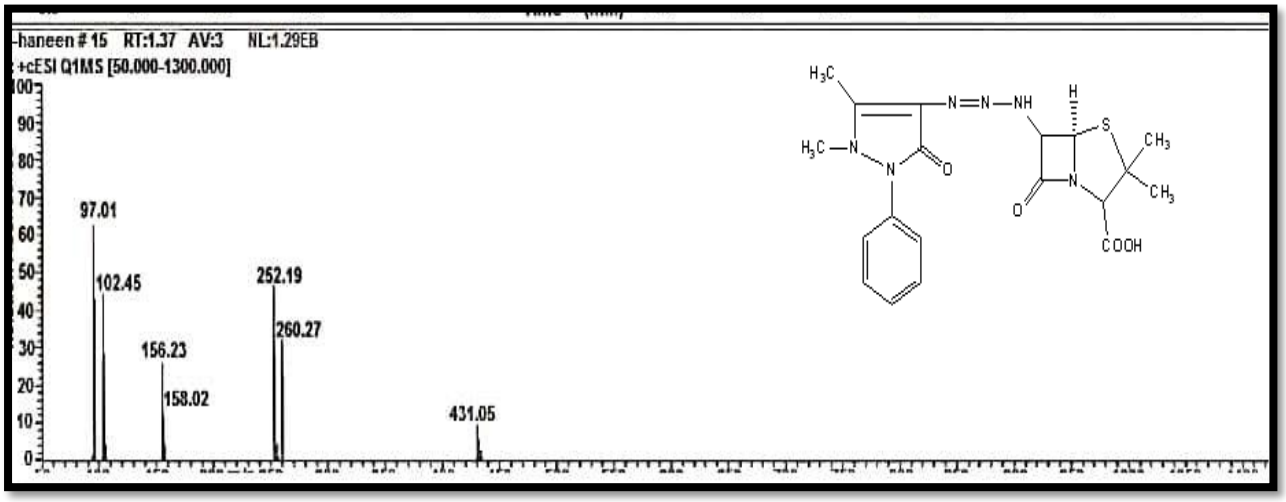

Fig. 4. Mass spectroscopy for ligand.

HNMR Spectroscopy

An NMR device was used to determine the type of hydrogen in the ligand as well as the composition of the ligand. The nuclear resonance spectra of the linker were measured, and a group of bands appeared in Fig. 5 exhibiting CH_3 (1.5 ppm, small, 6 hours; Kolganov *et al.* 2020), DMSO (3.5, 2.5 ppm; 2.3 ppm, d, h) and NH_3 (Ashutosh *et al.* 2018). This is supported by aromatics (7.5-8 ppm, m, 5 h) showing HNMR in Fig. 5 (Muhammad Ali *et al.* 2019).

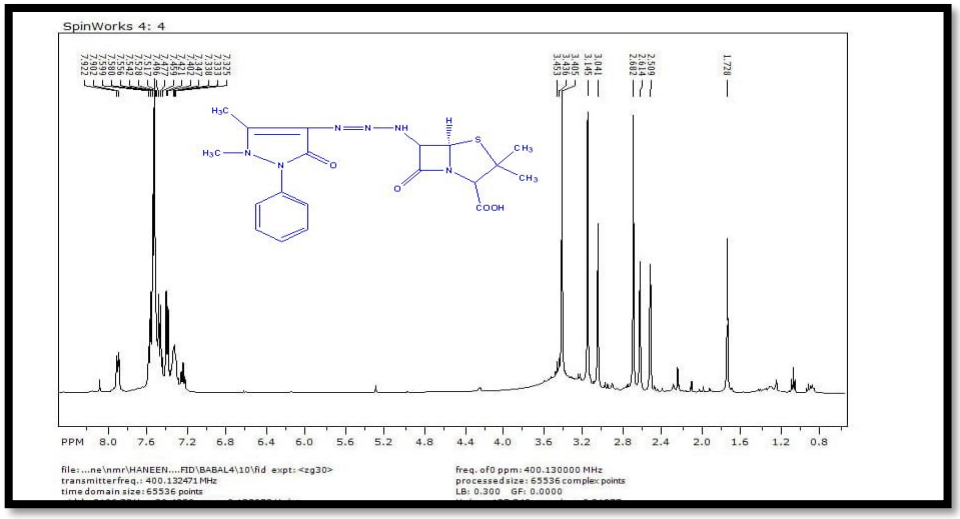

Fig. 5. HNMR for ligand.

FT-IR spectra of ligand

Strong bands can be observed in the FT-IR spectra of the synthesized ligands, L. In general, depending on the nature of the groups attached to it, the azo group/ absorption band emerges at the area of 1473 cm^{-1} (Farhan *et al.* 2022). The bands at 1541cm^{-1} for the C-C (Biswas & Umapathy 2000). For the synthesized ligands, the -lactam carbonyl group (C=O) was appeared at 1673 cm^{-1}. The other significant distinctive peak strong bands were

between 3600 and 3000 cm^{-1}. Due to the stretching vibrations V(O-H) and V(N-H), it is impossible to achieve sufficient resolution between bands due to OH and NH. Hence the band between 3500 and 2500 cm^{-1} is almost certainly attributable to OH and NH stretching in the FT-IR spectra (Fig. 6).

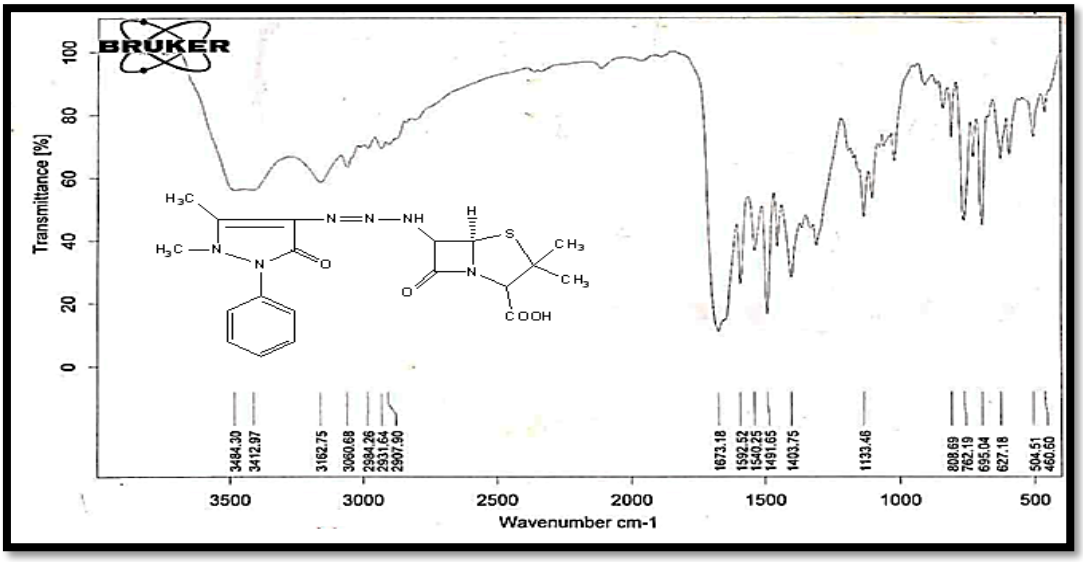

Fig. 6. FT-IR of ligand.

FT-IR Spectra of complex

Through the displacement of the azo group (N = N; 1403-1458 cm^{-1}; Biswas & Umapathy 2000) in all coordination compounds, this indicates the occurrence of coordination through them, as well as through the displacement of the carbonyl group present in the beta-lactam (1674-1701 cm^{-1}; Anacona *et al.* 2013). This indicates that the binding of the metal ion occurred through the carbonyl group. Other significant peaks observed in the FT-IR spectra are illustrated in Figs. 7, 8 and 9 and in Table 3.

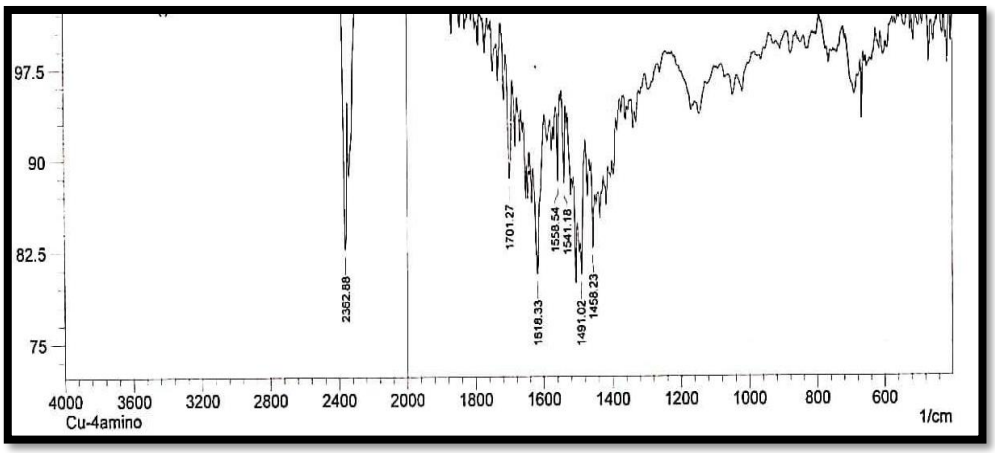

Fig. 7. Copper complex.

Table 3. FT-IR spectra of ligands and complexes.

Compound	C=O $_{lact}$	O-H	N=N-N	C=C	C=O car	C-HAR
Ll	1673	3454	1403	1540	1592	3152
$[Cd(L_1)_2(H_2O)_2]Cl_2$	1675	3412	1405	1589	1645	3171
$[Cu(L_1)_2(H_2O)_2]Cl_2$	1701	3416	1458	1558	1599	3167
$[Zn(L_1)_2(H2O)_2]Cl_2$	1629	3326	1405	1597	1654	3362

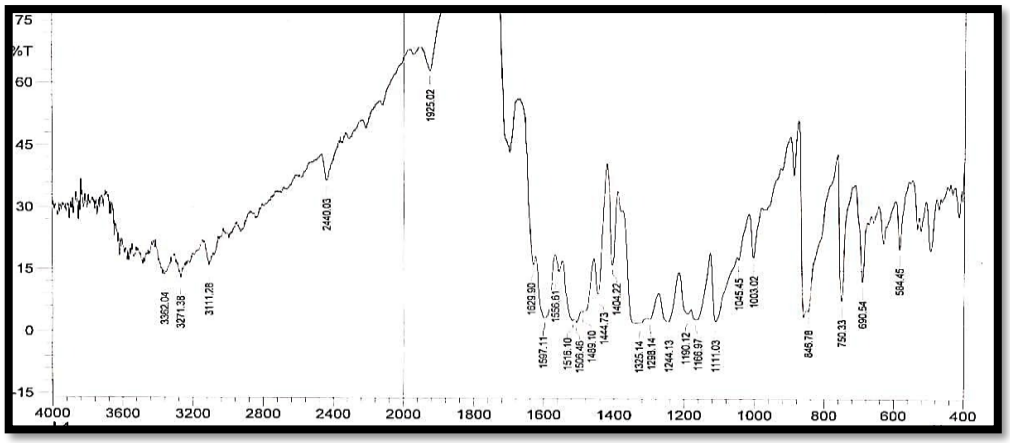

Fig. 8. Zinc complex.

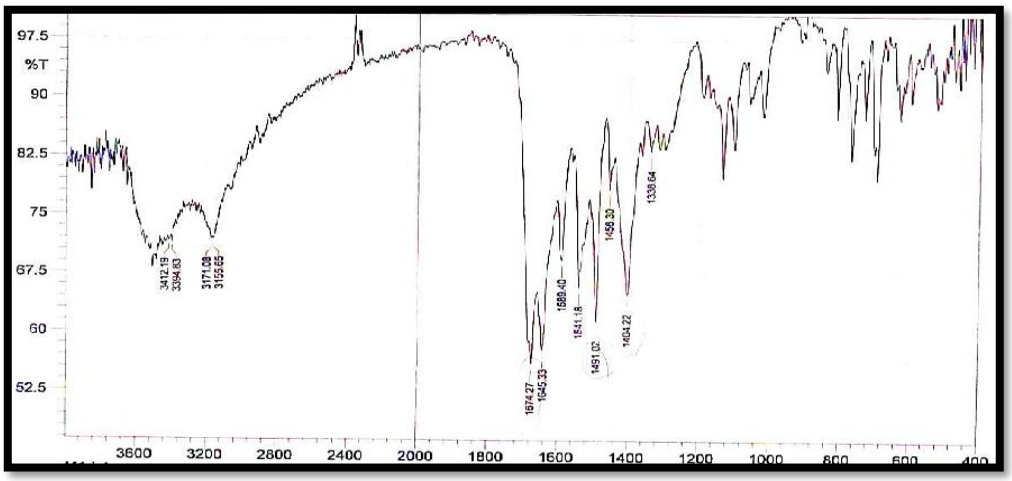

Fig. 9. Cadmium complex.

Spectrum of ligand and their complexes

Electron transition occurs due to the presence of double bonds and succession and returning to the aromatic ring. This leads to a transition of a kind π-π * (Fogel *et al.* 2007), and this transition appears in the peak. In addition, transitions of n-π^* (Kosower & de Souza 2006) occur as a result of the presence of electronic doublets. This peak appears in the Fig. 10. Furthermore, through the spectrum of UV-visible, it was observed that there is a displacement in all complexes as a result of the bonding between the transition metal and the ligands, (shown in Figs. 10, 11, 12, 13 and in Table 4).

Table 4. Electronic transition of L1 and there complexes

Compound	Absorption Band (nmλ)	Assignment
L1	230, 400	π-π*, n-π*
$[Cd(L_1)_2(H_2O)_2]Cl_2$	235,311	C.T
$[Zn(L_1)_2(H2O)_2]Cl_2$	240,400	C.T
$[Cu(L_1)_2(H_2O)_2]Cl_2$	235,310,640	π-π*, n-π*, d-d

Thermal analysis (TG)

Thermal characteristics of complexes were investigated using TGA studies. Fig. 14 depicts complex TG curves. The breakdown of the Cd (II) complex of L occurs in two phases (Ai *et al.* 2019). The complexes' stability to 2 °C signifies the start of the organic compound's degradation, which is related to the decomposition of the beta-lactam ring. The second stage begins at 2 °C of L, indicating the end of the organic compound's decomposition, leaving behind metal oxide as the end result. The presence of water was confirmed through the water exit through the thermal dissolution of the complex through the lost weight (shown in Tabe 5).

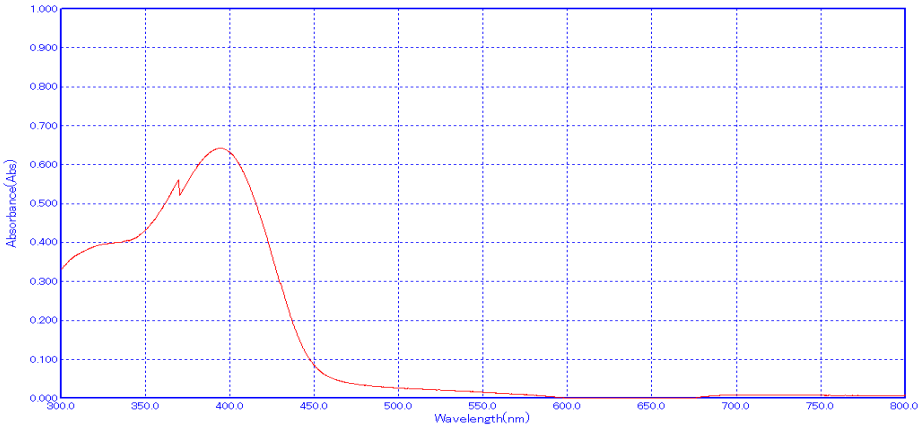

Fig. 10. Displaying a UV-visible for ligand.

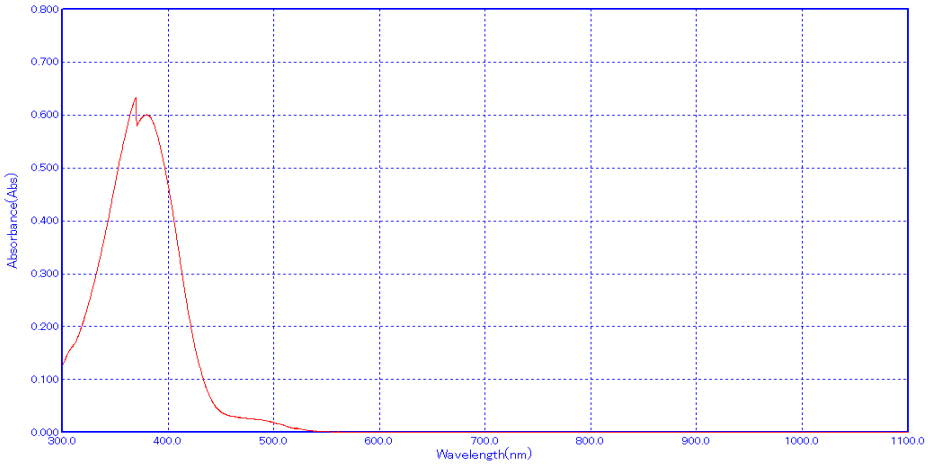

Fig. 11. UV-visible for cadium complex.

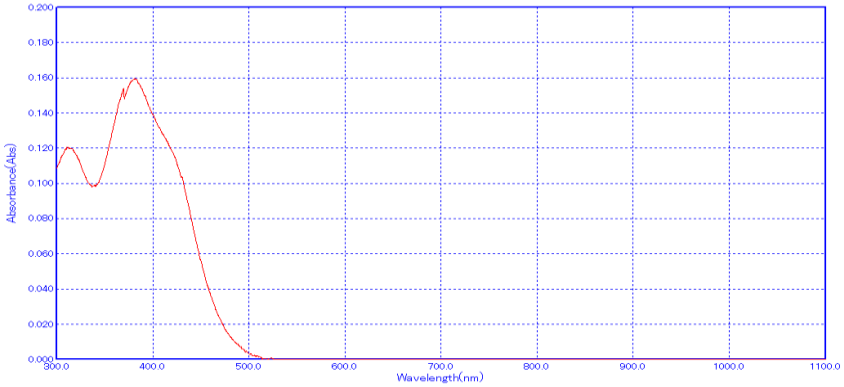

Fig. 12. Exhibiting a complex of UV-visible fo zinic complex.

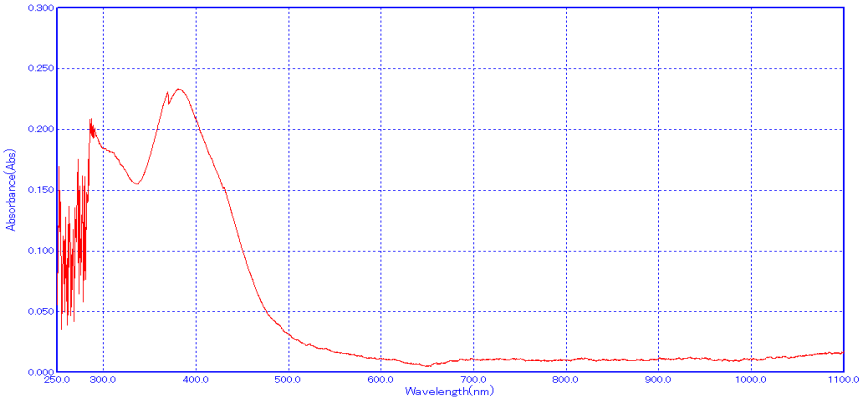

Fig. 13. A complex of copper.

Table 5. Thermal analysis.

Complexes	Beginning of decomposition (°C)	End of decomposition (°C)
$[Cd(L_1)_2(H_2O)_2]Cl_2$	38.55	406

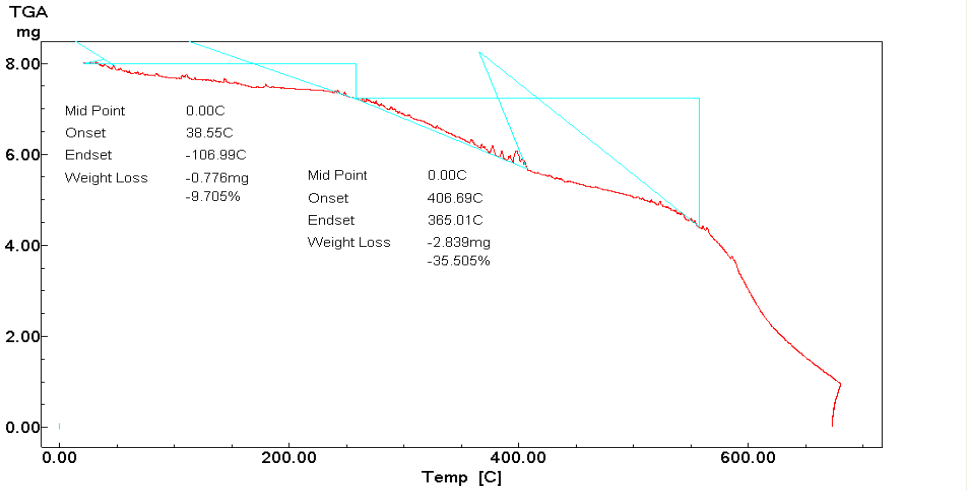

Fig. 14. TG curves of complex.

Atomic absorption

The atomic absorption approach was cast-off to calculate the percentage of Zn and Cd Cu (II) divalent ions in their complexes. The results reveal a good fit in Table 6.

Table 6. The Atomic absorption of complex.

Complexes	Theoretical value (%)	Practical value (%)
$[Cu(L_1)_2(H_2O)_2]Cl_2$	6.3	7.3
$[Zn(L_1)_2(H_2O)_2]Cl_2$	6.5	7.4
$[Cd(L_1)_2(H_2O)_2]Cl_2$	10.5	11.3

Conductivity

The molar conductivity of the initial ligand complexes was measured using ethanol at a concentration of 0.001 molar. The ionic character was inferred, and when the solutions were examined with silver nitrate, a positive result was given for this test, through the turbidity of the solution upon the addition of silver nitrate. The results shown in Tables 1-5.

Table 7. Molar conductivity values for complexes in ethanol solvent.

Complex	Molar conductivity
$[Cu(L_1)_2(H_2O)_2]Cl_2$	90
$[Zn(L_1)_2(H_2O)_2]Cl_2$	91
$[Cd(L1)_2(H_2O)_2]Cl_2$	99

The conductivity was measured and it turned out that it has a conductivity ratio of 1: 2. From the tables shown, it was noted that the two complexes have diamagnetic properties, and that one complex has par magnetic properties.

Biological Action of Ligands and Complexes

The bioactivity of the ligands and its complexes were examined for diverse bacteria utilizing an inhibitory strategy. The compounds exhibited inhibition zone (diameter) to the types of complexes against bacteria. The results displayed that the complexes have higher activity than the ligand under similar conditions. This may be due to the fact that chelation significantly reduces the polarity of the ion, primarily due to partial sharing of its positive charge with the donor groups and possible electron delocalization across the entire chelate ring (Table 9; Shehata *et al.* 2004). The experiment was also performed on another type of bacteria, exhibiting a negative result, since the compound works on the cell wall of the bacteria, destroying them. Since the gram-positive bacteria contain

the cell wall, therefore it inhibits them. The gram-negative bacteria does not contain a wall or has a thin wall, so the compound does not affect it.

Table 8. Magnetic susceptibility and for coordination complexes.

Compound	Mag. nature	Magnetic susceptibility	Hybridization
		μeff	
$[Zn(L_1)_2(H_2O)_2]Cl_2$	Di	0	sp3d2
$[Cu(L_1)_2(H_2O)_2]Cl_2$	Pa	1.07	sp3d2
$[Cd(L_1)2(H_2O)_2]Cl_2$	Di	0	sp3d2

Table 9. Biological activity for the ligand and complexes.

	Compound	Streptococcus
1	L	20
2	$[Cu(L_1)_2(H_2O)_2]Cl_2$	50
3	$[Cd(L1)_2(H_2O)_2]Cl2$	20
4	$[Zn(L_1)_2(H_2O)_2]Cl_2$	55

Fig 15. *Streptococcus* bacteria.

Fig. 16. *E. coli* bacteria.

CONCLUSION

The reaction between 4-amino anti pyrene and 6- amino penicillin acid in 1:1 mole product triazene ligand from Mass, ^{1}HNMR, FT-IR, UV. Through these techniques, the shape of the ligand was proven. The two-stranded ligand with the metal salt was formed, and its molar ratio was 2:1. The prepared ligand corresponded to Cu, Cd and Zn can be proven it by FT-IR, UV-Visible, molar conductance, magnetic susceptibility and Atomic Absorption. The complex shape was proposed and found to be octahedral by these techniques.

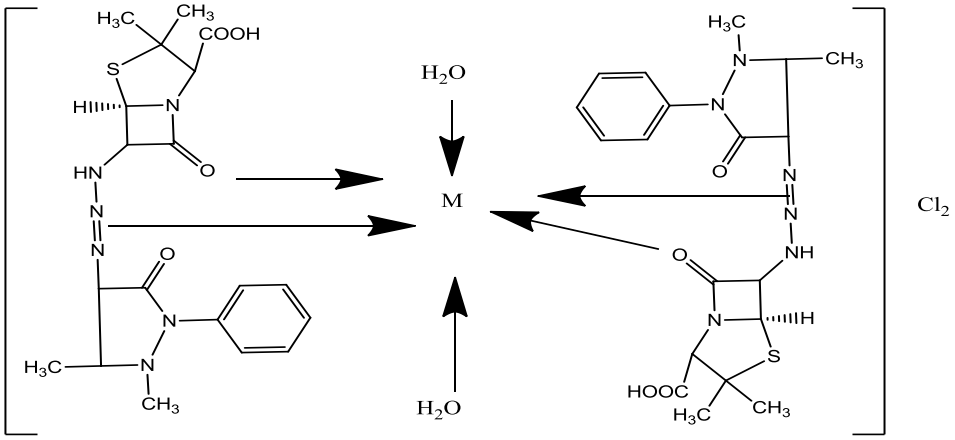

Fig. 17. The complex shape as octahedral by Mass, 1HNMR, FT-IR and UV.

The effect of the synthesized compounds on one species of harmful bacteria was investigated: The sensitivity of bacteria to the produced compounds was evaluated, with concentrations of the molecule as low as 0.001 molar in ethanol. These chemicals exhibited significant antibacterial efficacy and positive penetration in the bacterial cell. At the same concentration, compound 2 appeared to be the most active, with an inhibition zone of 50 mm.

REFERENCES

Ai, L, Hu, J, Ji, X & Zhao, H 2019, Structure confirmation and thermal kinetics of the inclusion of cis-jasmone in cyclodextrin. *RSC Advances*, 9(45): 26224-26229 .

Anacona, JR, Bravo, A & Lopez, ME 2013, Cefoperazone metal complexes: Synthesis and characterization. *Journal of the Chilean Chemical Society*, 58: 1520-1523.

Ashutosh, N, Gupta, AK & Sharma, V 2018, Interaction between irrigants commonly used in Endodontic practice and their characterization using 1H NMR Spectra. *International Journal of Research in Health and Allied Sciences*, 4: 15-19.

Ayakar, S & Yadav, GD 2019, Development of novel support for penicillin acylase and its application in 6-aminopenicillanic acid production. *Molecular Catalysis*.

Batchelor, FR, Doyle, FP, Nayler, JHC, Rolinson, GN 1959, Synthesis of penicillin: 6-Aminopenicillanic acid in penicillin fermentations. *Nature*. 183 (4656): 257-258, doi:10.1038/183257b0. PMID 13622762.

Biswas, N & Umapathy, S 2000, Structures, vibrational frequencies, and normal modes of substituted azo dyes: infrared, Raman, and density functional calculations. *The Journal of Physical Chemistry A*, 104(12): 2734-2745 .

Farhan, MM, Guma, MA, Rabeea, MA, Ahmad, I & Patel, H 2022, Synthesizes, characterization, molecular docking and in vitro bioactivity study of new compounds containing triple beta lactam rings. *Journal of Molecular Structure*, 1269: 133781 .

Fogel, Y, Kastler, M, Wang, Z, Andrienko, D, Bodwell, GJ & Müllen, K 2007, Electron-deficient N-heteroaromatic linkers for the elaboration of large, soluble polycyclic aromatic hydrocarbons and their use in the synthesis of some very large transition metal complexes. *Journal of the American Chemical Society*, 129(38): 11743-11749 .

Francisco, AP, Mendes, E, Santos, AR & Perry, MJ 2019, Anticancer Triazenes: From bio-precursors to hybrid molecules. *Current Design Pharmaceutical*, 25(14): 1623-1642, doi:10.2174/ 138161282566190617155749

Hui-nan, T, Wei-dong, G, Mou-Sheng, L & Yang Ya-ling, Y 2011, β21- cyclodextrin enhanced fluorometric method for determination of amoxicillin in dosage. *Chemical Research in Chinese Universities*, 27: 190-192.

Imam Pasha, S, Taqui, M, Shravan, KA & Nikhila V 2012, New visible spectrometric methods for the determination of amoxicillin Trihydrate in bulk drug and their formulations. *International Journal of Pharmacy and Industrial Research,* 2: 106-109.

Kolganov, AA, Gabrienko, AA, Chernyshov, IY, Stepanov, AG & Pidko, EA 2020, The accuracy challenge of the DFT-based molecular assignment of 13 C MAS NMR characterization of surface intermediates in zeolite catalysis. *Physical Chemistry Chemical Physics*, 22(41): 24004-24013.

Kosower, EM & de Souza, JR 2006, nπ-ct-π* Transitions: nπ* Transitions of the second kind. *Chemical Physics,* 324: 3-7 .

Marchesi, F, Turriziani, M, Tortorelli, G, Avvisati, G, Torino, F & De Vecchis, L 2007, Triazene compounds: mechanism of action and related DNA repair systems. *Pharmacological Research*, 56: 275–287. https://doi.org/10.1016/j.phrs.2007.08.003

Muhammad Ali, MA, Hamza Salman, H & Jasim, E 2019, Antioxidant activity of some newly prepared symmetrically azo dyes derived from sulfa drugs. *Asian Journal of Pharmaceutical and Clinical Research*, 12: 479-483

Naz, N & Iqbal, MZ 2011, Synthesis, spectroscopic and biological studies of transition metal complexes of novel Schiff bases derived from cephradine and sugars. Department of Chemistry, Lahore College for Women University, Lahore (Pakistan), ISSN 1013-5316, 23: 27-31.

Patrick, GL 2017, Medicinal Chemistry (6th ed.). Oxford, UK: Oxford University Press, 425 p. ISBN 978-0198749691.

Shehata, MR, Shoukry, MM & Barakat, M 2004, Coordination properties of 6-aminopenicillanic acid: binary and ternary complexes involving biorelevant ligands. J. Coord .Chem, 57(16), 1369-1386.

Suleymanov, AA, & Kay, S 2021, "Vinyl and Alkynyl Triazenes: Synthesis, reactivity, and applications. *Angewandte Chemie* 133: 6955-6965.

Zana Ibraimi, Z, Shedi, A, Hajrulai, Z, Mata, E & Murtezani, A 2013, Detection and risk assessment of beta lactam residues in Kosovo s milk using ELISA method. *International Journal of Pharmacy and Pharmaceutical Sciences*, 5: 446-450.

Bibliographic information of this paper for citing:

Hussein, HS, Said, MH, Shantaf, AH 2024, Preparation and characterization of cadmium (ll), zinc (ll) and copper (ll) ion complexes using new triazene ligands and study of their biological activity, Caspian Journal of Environmental Sciences, 22: 663-672.